

1
2
3
4
5
6
7
8
9
10
11
12
13
14
15
16
17
18
19

**Effect of Tropical Cyclones on the Tropical Tropopause Parameters observed using
COSMIC GPS RO data**

S. Ravindra Babu¹, M. Venkat Ratnam^{2*}, Ghouse Basha³, B.V. Krishnamurthy⁴ and
B.Venkatewsararao¹

¹Jawaharlal Nehru Technological University, Hyderabad, India.

²National Atmospheric Research Laboratory (NARL), Gadanki, India.

³Masdar Institute of Science and Technology, Abu Dhabi, UAE.

⁴CEBROSS, Chennai, India.

*vratnam@narl.gov.in , 08585-272123 (phone), 08585-272018 (Fax)

20 **Abstract**

21 Tropical cyclones (TCs) are deep convective synoptic scale systems and play an
22 important role in modifying the thermal structure, tropical tropopause parameters and hence
23 stratosphere-troposphere exchange (STE) processes. In the present study, high vertical
24 resolution and high accuracy measurements from COSMIC Global Positioning System (GPS)
25 Radio Occultation (RO) measurements are used to investigate and quantify the effect of
26 tropical cyclones that occurred over Bay of Bengal and Arabian Sea in last decade on the
27 tropical tropopause parameters. The tropopause parameters include cold point tropopause
28 altitude (CPH) and temperature (CPT), lapse rate tropopause altitude (LRH) and temperature
29 (LRT) and the thickness of the tropical tropopause layer (TTL), that is defined as the layer
30 between convective outflow level (COH) and CPH, obtained from GPS RO data. From all the
31 TCs events, we generate the mean cyclone-centered composite structure for the tropopause
32 parameters and removed from climatological mean obtained from averaging the GPS RO data
33 from 2002-2013. Since the TCs include eye, eye walls and deep convective bands, we
34 obtained the tropopause parameters based on radial distance from cyclone eye. In general,
35 decrease in the CPH in the eye is noticed as expected. However, as the distance from cyclone
36 eye increases by 300 km, 400 km, and 500 km an enhancement in CPH (CPT), LRH (LRT)
37 are observed. Lowering of CPH (0.6 km) and LRH (0.4 km) values with coldest CPT and
38 LRT (2-3 K) within the 500 km radius from the TC centre is noticed. Higher (2 km) COH
39 leading to the lowering of TTL thickness (2-3 km) is clearly observed. There exists multiple
40 tropopause structures in the profiles of temperature obtained within 100 km from centre of
41 TC. These changes in the tropopause parameters are expected to influence the water vapour
42 transport from troposphere to lower stratosphere and ozone from lower stratosphere to the
43 upper troposphere and hence STE processes.

44 **Key words:** Tropical tropopause, tropical cyclones, COSMIC GPS RO measurements.

45

46 **1. Introduction**

47 Tropical Cyclones (TCs) are one of the most dangerous natural and deep convective
48 synoptic scale systems that occur throughout the tropical region globally (Emanuel 2005).
49 Every year, they cause considerable loss of life and damage to property. India has a long
50 coastline, which is prone to very severe cyclone formations in the Arabian Sea (AS) and Bay
51 of Bengal (BoB). Over the Indian region, these TCs occur during the pre-monsoon (April-
52 May), early monsoon (June) and post monsoon (September - November) seasons (Pattnaik et
53 al., 2008). They persist for a few days to weeks and have large convective activity around the
54 eye with a horizontal scale of hundreds of kilometres. During the developing stage of TCs, a
55 large drop in its central pressure occurs and the most extreme vertical velocities are usually
56 observed. TCs contain large amounts of water vapour, energy and momentum, and transport
57 water vapour and energy to the upper troposphere and lower stratosphere (UTLS) region.
58 Hence, TCs play a very important role in affecting the thermal structure and dynamics of
59 UTLS. The concentration of the water vapour transported to the stratosphere is controlled by
60 the cold temperatures present at the tropopause (Fueglistaler et al., 2003). The life time and
61 size of cyclones also might be affecting the tropopause parameters on the regional scales
62 (Cairo et al., 2008). There could be a possibility that TCs lift and cool the tropopause more
63 than other meso- scale systems (Romps and Kuang, 2009). It is well known that the intensity
64 and frequency of TCs have increased in recent years (Emmanuel, 2005; Webster et al., 2005).

65 The tropopause, which is the boundary between troposphere and stratosphere, plays a
66 crucial role in the exchange of mass, water vapour and other chemical species between the
67 two atmospheric regions (Holton et al., 1995). Most of these exchanges (water vapour to the
68 lower stratosphere and ozone to the upper troposphere) take place around tropopause only
69 and as such it is very important to study and understand the physical processes occurring
70 around the tropopause region. The tropopause itself varies temporally and as well as spatially.

71 Generally, radiosonde data have been used to study the tropopause parameters and their
72 characteristics (e.g., Randel et al., 2000; Seidel et al., 2001). However radiosonde data is not
73 available over oceans particularly during severe atmospheric conditions like TCs. Thus,
74 obtaining the tropopause characteristics during TCs remained a daunting task. However, the
75 availability of Global Positioning System (GPS) Radio Occultation (RO) measurements with
76 high vertical resolution, high accuracy and all-weather capability made it possible to study
77 the tropopause characteristics over globe including over oceans. Several studies showed that
78 the GPS RO measurements are well suited for studying the severe storms (Pommenreau and
79 Held, 2007; Corti et al., 2008; Romps and Kuang, 2009; Biondi et al., 2013).

80 A few studies have been carried out relating the TCs and its link to the UTLS as well
81 as tropopause parameters. Studies include the thermal and dynamical structure of UTLS
82 during TC (Koteswaram, 1967), horizontal and vertical structure of temperature in the
83 cyclone (Waco, 1970), temperature and ozone variations in a hurricane (Penn, 1965),
84 troposphere-stratosphere transport and dehydration in cyclones (Danielsen, 1993), UTLS
85 structure during TCs using AIRS and MLS measurements (Ray and Rosenlof, 2007), RO
86 bending angle anomalies during tropical cyclones (Biondi et al., 2011), thermal structure of
87 intense convective clouds derived from GPS RO (Biondi et al., 2012), estimating the TC
88 cloud top height and vertical temperature structure using GPS RO measurements (Biondi et
89 al., 2013), and observations of temperature in the UTLS of tropical weather disturbances
90 (Davis et al., 2014). Note that above list is only indicative but not exhaustive. Recently
91 Emmanuel et al. (2013) showed that the modulations of the cold point temperature influence
92 the maximum potential intensity of tropical cyclones and tropical cyclone activity. However,
93 the effect of deep convection associated with the TCs on the tropopause parameters is not yet
94 fully understood.

95 The main objective of the present study is to investigate the spatial variation of
96 tropopause parameters such as cold point tropopause altitude (CPH) / temperature (CPT),
97 lapse rate tropopause altitude (LRH) / temperature (LRT), convective outflow level altitude
98 (COH) and TTL thickness with respect to TC centre during entire TC period. Vertical
99 structure of temperature and tropopause parameters within the 5° radius away from the
100 cyclone centre during TC period is also presented. The water vapour variability in the vicinity
101 of TC is also investigated. The details of the data used for the present study are mentioned in
102 Section 2. Methodology for obtaining tropopause parameters during TC period is mentioned
103 in Section 3. Results and discussion are presented in Section 4. Finally, summary and
104 conclusions drawn from the present study are presented in Section 5.

105 **2. Database**

106 **2.1. COSMIC GPS RO data**

107 The temperature profiles obtained from the Constellation Observing System for
108 Meteorology, Ionosphere, and Climate (COSMIC) GPS RO over the BoB during the TC is
109 utilised for the present study. The GPS RO data were downloaded from COSMIC Data
110 Analysis and Archive Centre (CDAAC) website ([http://cosmic-
111 io.cosmic.ucar.edu/cdaac/index.html](http://cosmic-io.cosmic.ucar.edu/cdaac/index.html)). COSMIC GPS RO is a joint Taiwan – U.S. mission,
112 constellation of six microsatellites equipped with GPS receivers (Anthes et al., 2008). These
113 satellites are launched in early 2006 and started providing data from April 2006. During its
114 initial phase, all the six satellites were not fully configured so as to get uniform distribution of
115 occultations. Thus, data from 2007 to 2013 have been used for the present study. It provides
116 2000-2500 occultations for a day over entire globe. Details of temperature retrieval from
117 bending angle and refractivity profile obtained from GPS RO sounding are presented
118 elsewhere (Kursinski et al., 1997; Kuo et al., 2004; Anthes et al., 2008; Schreiner et al.,
119 2010). For the present study we use level 2 atmPrf temperature profiles to calculate the

120 tropopause parameters during the TCs. In addition, we also used CHALLENGING Minisatellite
121 Payload (CHAMP) GPS RO data that are available between the years 2002 to 2006. This
122 complete data (2002 to 2013) is used to generate the background climatology of tropical
123 tropopause parameters over North Indian Ocean. The vertical resolution of the temperature is
124 200 m and accuracy is 0.5 K (7-25 km) Note that this data is validated with variety of
125 techniques including GPS radiosonde and found very good match particularly in the UTLS
126 region (Rao et al., 2009).

127 **2.2. TCs best tracks**

128 We have taken the TC track information (TCs best tracks) data from the India
129 Meteorological Department (IMD) for the period 2007 to 2013. Though GPS RO data is
130 available between 2002 and 2006 from CHAMP GPS RO, we have not utilised it for
131 estimating the tropopause parameters during TC as the number of occultations from this
132 single satellite are too sparse (maximum 250-300 occultations over entire globe). TCs track
133 information includes TC name, dates, centre latitude and longitude, cyclone intensity (CI)
134 and MSL pressure of the TC at every 3 h intervals during the formation of the TC. During
135 this period (2007 to 2013), around 44 TCs have formed over North Indian Ocean. For the
136 present study, we consider only the TCs which are having life time of minimum 4 days and
137 more. From these 44 TCs we selected 16 TCs based on life time of TCs to investigate the
138 effect of TCs on the tropical tropopause parameters. The tracks of all the TCs used for the
139 present study are shown in Figure 1 and different colours indicate TCs occurred in different
140 years. Note that only 2 TCs have formed over AS and rest all formed over BoB. Only one TC
141 that formed over BoB have crossed the Indian land mass and have strengthen again when it
142 reached AS. The details of TC such as name, grade, CI (Cyclone Intensity) number as
143 designated by IMD, life time, central latitude and longitude (position) of the cyclone where

144 lowest pressure and highest wind speed are observed with estimated pressure drop are shown
145 in Table 1. Details of the acronyms used in this table are provided in sub-section 3.2.

146 **3. Analyses procedure**

147 **3.1. Estimation of different tropopause parameters**

148 The tropopause is defined in different ways (Highwood and Hoskins, 1998) and the
149 most commonly used one in the tropics is the cold point tropopause. The CPH is defined as
150 the altitude of the temperature minimum that exists between the troposphere and stratosphere.
151 Another one is LRH defined by World Meteorological Organization (WMO) (1957) as, ‘the
152 lowest level at which the lapse rate decreases to 2 K/km or less provided that the average
153 lapse rate between this level and all higher levels within 2 km does not exceed 2 K/km.’

154 In recent years, the study of the tropopause over tropics has led to the concept of a
155 Tropical Tropopause Layer (TTL) (Highwood and Hoskins, 1998; Gettleman and Birner,
156 2007; Fueglistaler et al., 2009), which is the transition region between the convective-
157 radiative equilibrium of the troposphere and the stratosphere. In this transition region both
158 stratospheric and tropospheric processes interact. The top of the TTL is marked by the CPH
159 and the base by the level of the top of all the major convective outflows, named as convective
160 tropopause altitude (COH) and the altitude difference between CPH and COH is the TTL
161 thickness. A minimum in potential temperature gradients is identified as COH following
162 Gettleman and Foster (2002). Note that it closely matches with the divergence profile
163 obtained from Mesosphere Stratosphere Troposphere (MST) radar observations (Mehta et al.,
164 2008). All these parameters (CPH, CPT, LRH, LRT, COH and TTL thickness) are estimated
165 for each profile of GPS RO during the entire TC life time. In order to estimate the effect of
166 TCs on the tropopause parameters, the background of all the tropopause parameters is
167 obtained by averaging the data from 2002 to 2013 (climatology) with exclusion of the days
168 of the TCs. These climatological values are grouped at $2.5^\circ \times 2.5^\circ$ grids. There could be day-

169 to-day to the inter-annual variability in the observed climatological tropopause parameters.
170 Since large data (14 years) has gone through it, we assume variability less than solar cycle is
171 nullified if not removed completely.

172 **3.2. Classification of the TCs**

173 Effect of the TCs on the tropopause parameters mainly depends on the intensity of the
174 cyclone. Tropical cyclone intensity is defined by the maximum mean wind speed over open
175 flat land or water, sometimes referred to as the maximum sustained wind that will be
176 experienced around the eye-wall of the cyclone. The low pressure system over Indian region
177 is classified based on the maximum sustained winds speed associated with the system and the
178 pressure deficit/ number of closed isobars associated with the system. The pressure criteria
179 are used when the system is over land and wind criteria is used when the system is over the
180 sea (IMD). Based on 10 minutes maximum sustained wind speed, IMD has defined various
181 stages of the TC. It is named as low pressure when the maximum sustained wind speed at the
182 sea surface is <17 knots/32 kmph, Depression (D) (17–27 knots/32-50 kmph), Deep
183 Depression (DD) (28–33 knots/51-59 kmph), Cyclonic Storm (CS) (34-47 knots/60-90
184 kmph), Severe Cyclonic Storm (SCS) (48-63 knots/90-110 kmph), Very Severe Cyclonic
185 Storm (VSCS) (64–119 knots/119-220 kmph) and Super Cyclonic Storm (SuCS) (>119
186 knots/220 kmph). As an example, the TC Nargis is chosen to show the different stages of TC
187 and also its pressure and wind speed. The TC ‘Nargis’ originated as a depression formed over
188 southeast BoB at 0300 UTC on 27 April 2008. From Table 1 it is clear that this cyclone
189 comes under the category VSCS which has CI of 5. The observed IMD track of the VSCS
190 Nargis is shown in Fig. 1 (green line). This system slightly moved north eastwards and
191 intensified into a cyclone at 00 UTC of 28 April. It remained stationary for some time and
192 further intensified into a SCS at 0900 UTC of 28 April and into a VSCS grade, as classified

193 by the IMD at 0300 UTC of 29 April (Pattnaik and Rama Rao, 2008). Further it moved
194 eastward and crossed the coast of Myanmar on 2 May at 0600 UTC.

195 The IMD reported maximum wind speed and minimum SLP of the TC Nargis are
196 shown in Fig. 2(a). Note that highest wind speed (~90 knots) and lowest pressure (~960 hPa)
197 are noticed on 02 May. The interpolated outgoing long-wave radiation (OLR), which is
198 considered as proxy for tropical deep convection, obtained from NOAA satellite on 28 April
199 2008 is shown in Fig. 2(b) along with the track of the cyclone provided by IMD. Black
200 circles are drawn to show the 500 km, 1000 km, 1500 km and 2000 km radius from the TC
201 center. Note that this cyclone was stationary on 28 April and the minimum OLR (maximum
202 convection) which was as low as 90 W/m^2 , lay over the region within 500 km and extended
203 to south east and west side of cyclone track within 1000 km. The monthly mean of CPH for
204 the month of April is shown in Fig. 2(c) and small black circle show the TC Nargis centre
205 observed on 28 April 2008. An interesting feature to be noticed is enhancement of CPH
206 around 25°N over Indian region than equatorial latitudes which is well reported earlier
207 (Venkat Ratnam et al., 2005). This feature is commonly observed over Indian region. Note
208 that latitudinal variation of 500 m can be observed if we consider 2000 km from the centre of
209 cyclone. In order to avoid this latitudinal variation, we restrict our discussion within 1000 km
210 from the cyclone centre hereafter.

211 The COSMIC RO data obtained for each day during the cyclone period are separated
212 based on IMD cyclone best track data and calculated the tropopause parameters for each
213 individual temperature profile. Since IMD based TC track data is available at 3 h intervals,
214 we considered the middle of the coordinates (latitude and longitude) of particular day of TC
215 as the centre of TC for that day. Based on these centres we calculated the distance from the
216 TC centre for each individual RO available on particular TC day at intervals of 250 km up to
217 1000 km.

218 **4. Results and discussion**

219 **4.1. Tropopause parameters observed during VSCS Nargis**

220 The locations of all the COSMIC GPS RO observations on 28 April 2008 are shown
221 (white circles) in Fig. 2(b). There were about 13 occultations that occurred within 1000 km
222 from the centre of the cyclone. All the tropopause parameters mentioned in section 3.1 are
223 estimated for each of these profiles and climatological values were subtracted for estimating
224 the effect of the TCs on the tropopause parameters. Typical example of cyclone-centred
225 tropopause parameters obtained from the COSMIC GPS RO profiles during TC Nargis on 28
226 April 2008 is shown in Figure 3 (a) CPH, (b) LRH, (c) CPT, (d) LRT, (e) COH and (f) TTL
227 thickness, respectively and Black circles are drawn to shown the 250 km, 500 km, 750 km
228 and 1000 km away from TC centers. Though it is difficult to draw any conclusion from this
229 figure as occultations are sparse, it is clear that CPH and LRH are slightly lower (~ 17.25 km)
230 within 500 km and higher (>17.5 km) away when compared to the CPH and LRH around
231 1000 km. There is no substantial difference in the CPT and LRT within 500 km of TC in this
232 example. However, COH is a little higher (~ 14 km) within 500 km and slightly lower away
233 from it and TTL thickness is small (< 4 km) within 500 km from the centre of TC Nargis.
234 This suggests that the TC affects the tropopause parameters. Note that the variations observed
235 away from 500 km, mainly over land, can be partly attributed to the latitudinal change itself
236 which will be discussed further in the next sections.

237 Note that the GPS RO estimated temperature near the tropopause during cyclone
238 activity is expected to be biased with the assumption of dry atmosphere as sometimes water
239 vapour is being pumped up to the tropical tropopause. However, note that we could notice
240 similar change in bending angle and hence refractivity which is combination of temperature
241 and water vapour. In the simulations reported in Rao et al. (2009), one can notice that change
242 in the temperature is not that sensitive when compared to the pressure and water vapour.

243 Since, the changes are found to be up to 4-5 K, we expect these are meaningful even after
244 considering expected larger bias during disturbed weather conditions. More details of
245 COSMIC temperature during Cyclone period can be found in Biondi et al., (2011).

246 **4.2. Spatial variations of tropopause parameters from the centre of TC**

247 In this sub-section, the spatial variations of tropopause parameters from the cyclone
248 centre for different intensities of TC are presented. From the example of Nargis it is clear that
249 we have less number of occultations for a single TC day and hence it is difficult to describe
250 the tropopause characteristics away from the TC centre. For getting more data points for
251 statistically significant results, we have separated COSMIC RO data based on TC intensity
252 from all the 16 TCs. When we separated these based on TC intensity wise with respect to
253 their distance from the TC centre there are 381, 727, 1124, 481 and 865 occultations for D,
254 DD, CS, SCS and VSCS, respectively. From these profiles, we made a 250 km x 250 km grid
255 of tropopause parameters based on TC centre for all TC intensities. After going through the
256 detailed analysis, no significant difference in the tropopause parameters between D and DD,
257 CS and SCS was noticed. So, we have combined the observations obtained during those
258 periods, respectively. Since there is no significant difference in the tropopause parameters
259 during D and DD we have not shown these here.

260 Figure 4 shows cyclone-centered composite of (a) CPH, (b) LRH, (c) CPT, (d) LRT,
261 (e) COH and (f) TTL thickness for the cases of CS and SCS. From the figure it is clear that
262 the south west side of the area up to 1000 km radius from the TC centre the CPH (Fig 4a) and
263 LRH (Fig 4b) is lower than the north side of the TC centre. However, colder tropopause
264 temperatures are clearly observed within 1000 km in case of CPT (Fig 4c) and LRT (Fig 4d).
265 A 10 K difference in the CPT and LRT can be noticed from the TC centre to the north side.
266 Very interestingly COH is much higher over 1000 km and also towards south side from the
267 TC centre with maximum altitude of around 15 km (Fig 4e) leading to a smaller TTL

268 thickness (Fig. 4f). Note that TTL thickness is less than 3 km within 500 km from the centre
269 of TC and up to 1000 km in the southern side. These different variations in the tropopause
270 parameters might be due to two reasons. One may be due to distribution of convection during
271 developing stages of TCs such as depression and deep depression on the south side of the TC
272 centre which moved north-west side. Another reason, at least in part, can be attributed to the
273 latitudinal variation. However, we found very low values of CPH within the 500 km radius
274 from the TC centre. Similar variations are observed when we separated the TC based on
275 different intensities (figures not shown). Thus, in general, we observed lowering of CPH and
276 LRH values with coldest CPT and LRT within the 500 km radius from the TC centre. Higher
277 COH leading to lowering of TTL thickness is clearly observed. Higher COH within the 500
278 km from the TC centre suggests that maximum convective outflow reached higher altitude.
279 At the same time lowering the CPH, leading to the small TTL thickness, within the TC centre
280 is observed probably due to the subsidence. In order to quantify the effect of TCs on the
281 tropopause parameters more clearly we have obtained anomalies by subtracting the
282 tropopause parameters observed during TC from the background climatological tropopause
283 parameters.

284 Figure 5 shows mean difference of cyclone-centered tropopause parameters from the
285 background climatology observed in CPH, LRH, CPT, LRT, COH and TTL thickness. Note
286 that this figure is the composite of the all the tropopause parameters irrespective of the TC
287 intensity. Thus, some differences between Figure 4 and Figure 5 can be expected. In general,
288 the CPH (LRH) is lowered by 0.6 km (0.4 km) in most of the areas within the 1000 km radius
289 from the TC centre and CPT (and LRT) is colder by 3-4 K. Note that this decrease in the
290 CPH is not uniform over 1000 km radius from the centre. Throughout the area 1000 km from
291 center the temperature is more or less colder or equal to the climatological value in both
292 CPT/LRT. COH has increased up to 2 km within 500 km from the TCs and at some areas up

293 to 1000 km. TTL thickness is reduced by 2 km within 500 km from the TC centre and over
294 some areas up to 1000 km. Note that this decrease in TTL thickness is not only because of
295 pushing up of the COH but also decrease of CPH. It is worth quoting the recent findings of
296 Biondi et al. (2015) where they reported a decrease in the temperatures of 3-4 K and
297 reduction in the TTL thickness to 2-3 km over north Indian basin. Our findings exactly match
298 with their reports for Indian region.

299 **4.3. Spatial variations of water vapor from the centre of TC**

300 Deep convection is expected to reach up to the tropopause altitude and sometimes
301 above during the TCs leading to the penetration of water vapor to the lower stratosphere. At
302 the same time chances of pushing down the ozone from the lower stratosphere leading to
303 lower CPH (subsidence) is also expected leading to the STE processes. Though not
304 completely relevant to the present study, it is worth to recall recent results by Škerlak et al.
305 (2014), where it was shown quantitatively that maxima of STE are located over the storm
306 (cyclone) track regions in the North Atlantic and North Pacific during all seasons (except
307 summer) with an averaged mass flux of approximately $500 \text{ kg km}^{-2} \text{ s}^{-1}$ from the stratosphere
308 to the troposphere and approximately $300 \text{ kg km}^{-2} \text{ s}^{-1}$ in the opposite direction. It will be
309 interesting to investigate how these numbers compare for TC over Indian region. Since GPS
310 RO also provides information on water vapor (Kishore et al., 2011), we have investigated
311 further the effect of TCs on the vertical distribution of water vapor. Cyclone centre –
312 composite of averaged RH observed during all the TCs irrespective of TC intensity in the
313 layer 0-5 km, 5-10 km and 10-15 km using COSMIC GPS RO wet-profiles is shown in
314 Figure 6(a)-(c), respectively. Note that above these altitudes, water vapour is not sensitive in
315 the GPS RO measurements. In general, larger RH values are noticed in the south-eastern side
316 of the TCs in the lower layer (0-5 km) and throughout south side of the TC in the layer 5-10
317 km. Higher RH is noticed within 500 km from the TC centre. Interestingly, high RH values

318 of 70% or more are noticed on the eastern side of TC in the layer 10-15 km. Thus, it is clear
319 that deep convection prevailing during the TC within 500 km from the centre of TC can
320 penetrate to the lower stratosphere through the tropopause. The higher RH values observed in
321 the layer 10-15 km may be due to the upper level anti-cyclonic circulation over the cyclones.
322 Ray and Rosenlof (2007) reported higher water vapour mixing ratios to the east of the
323 cyclone centre for TCs over Atlantic and Pacific Oceans and found averaged water vapour is
324 enhanced by 30-50 ppmv or more within 500 km of the eye compared to the surrounding
325 average water vapour mixing ratios. Our results match well with these. Note that Biondi et al.
326 (2015) reported 30-50% of the time overshooting of the convection during TCs strongly
327 supporting our findings. At the same time, Midya et al., (2012) reported that over BoB and
328 AS the total column ozone (TOC) decreases steadily before and during the formation of a TC,
329 followed by a more or less increasing trend after dissipation of the cyclone. A very recent
330 case study by Das et al., (2015, submitted manuscript) also confirms the intrusion of
331 stratospheric air into the upper and middle troposphere during the passage of tropical cyclone
332 Nilam. It will be interesting to see the variability of ozone during the same time for all the
333 cyclones presented here to investigate the STE processes away from the TC center.

334 From the above, in general, it can be concluded that tropical tropopause is
335 significantly affected by the TCs. The effect is more pronounced within 500 km from the
336 centre of TC. Note that TCs have eye, eye wall, rain bands, convective cloud tops, strong
337 updrafts and cirrus deck, all occurring in the range of 500 km to 1000 km from the TC
338 centre. From the above results, we expect a significant effect of the TCs on the tropopause
339 parameters could be felt up to 500 km from the TC centre. We have further investigated the
340 effect of TCs on the thermal structure of UTLS region and the results are presented in the
341 next section.

342 **4.4. Vertical thermal structure of UTLS within 500 km from TC centre**

343 We considered the GPS RO with respect to the IMD best track data and took ± 1 h time
344 window of co-located RO profiles with respect to IMD best track time for every 3h. Based on
345 this we calculated the distance from the TC centre. We classified them with respect to
346 distance from the centre as 100 km, 200 km, 300 km, 400 km, and 500 km respectively. There
347 were 90 GPS RO occurring within 500 km and when we separated them at 100 km steps
348 there were 7, 11, 20, 20 and 32 profiles, respectively. Figure 7 shows mean vertical structure
349 of temperature with respect to distance within 500 km at steps of 100 km from TC centre
350 along with standard error. Enlarged portion in the Figure 7 shows vertical structure of the
351 temperature within the UTLS region from 16 -18 km. Here we considered ± 1 h time window
352 of co-located RO profiles with respect to IMD cyclone best track data for getting thermal
353 structure over TC period. Note that this is a better time window resolution than the earlier
354 reported 3h time window by Biondi et al., (2013) for describing the thermal structure during
355 cyclone period. In general, no significant difference in the temperature structure within 500
356 km from TC centre below 14 km is noticed. This is mainly due to the synoptic nature of
357 convection within the 500 km radius from the TC centre. Generally, in the troposphere below
358 approximately 14 km the radiative cooling balances the latent heat release by convection.
359 However, large variation in the mean temperature structure can be noticed above 14 km. This
360 is mainly due to balancing between the radiative heating and the stratosphere-driven
361 upwelling above 16 km. Strong updrafts around the eye wall and down drafts, subsidence
362 near the eye, and formation of the cirrus clouds might change the temperature structure in the
363 UTLS region strongly. It is interesting to notice lowering of tropopause altitudes with colder
364 temperatures in the profiles obtained within 100 km, followed at 300 km, 200 km and 400
365 km. It indicates that rain bands are of the size of roughly 100 km . There exists a temperature
366 difference of 5K in the UTLS region in the profiles that occurred within 100 km from the
367 profiles that occurred away of 400 km. These are statistically significant differences as the

368 error bars do not mix with each other for the profile that occurred within 100 km to rest of the
369 profiles. Warmer temperatures are also visible in the lower stratosphere in the profiles that
370 are obtained within 100 km when compared to those occurred away. Multiple tropopause
371 structures are clearly visible in the profiles that occurred within 100 km from the TC though
372 number of profiles available is small. These multiple tropopauses are similar to that are
373 double tropopauses observed by Corti et al. (2008), Biondi et al. (2011) and Davis et al.
374 (2014). The cause for these multiple tropopauses might be either due to clouds (Biondi et al.,
375 2013) or wave activity or cirrus or ozone (Mehta et al., 2011) which demands separate
376 investigation.

377 We also calculated the tropopause parameters with respect to 100 , 200, 300, 400, and
378 500 km away from the TC centre respectively. Figure 8 shows the mean tropical tropopause
379 parameters of CPH, CPT, LRH, LRT, COH and TTL thickness observed from the profiles
380 that are available within the 500 km radius from the TC centre. In general, CPH (CPT)
381 increases (decreases) as we move away from the TC centre within 500 km (except at 200 km
382 in case of CPH) (Fig. 8a). There exists a difference of 0.4 km (3 K) in the CPH (CPT) within
383 500 km from centre of TC. Similar variability in the LRT is observed but not in LRH (Fig.
384 8b). An inverse relation between LRH and LRT is noticed but not in CPH and CPT. A nearly
385 2 km decrease in COH is clearly noticed (Fig.8c) when we move away from the TC centre
386 leading to the increase in the TTL thickness of 3 km (Fig. 8d). Note that lowering of CPH
387 (may be due to the presence of subsidence and strong downdrafts) in the eye region and
388 higher COH leading to lowering of TTL thickness within 100 km from the TC centre is again
389 noticed. Most of the overshooting convection may occur within the 200 km and top of the
390 convection may be lifting the tropopause higher. An additional 1 km of lowering of the TTL
391 thickness within 100 km when compared to 500 km away from TC centre is mainly coming

392 from lowering of CPH. Thus, decrease in TTL thickness is the combination of pushing up of
393 COH and lower of CPH.

394 **5. Summary and conclusions**

395 In the present communication, we investigated and quantify the effects of tropical
396 cyclones that occurred between 2007 and 2013 on the tropical tropopause parameters
397 obtained from simultaneous high vertical resolution and high accuracy COSMIC GPS RO
398 measurements. TCs are categorized based on their intensity as their effect on the thermal
399 structure and thus tropopause parameters will be different for different intensities. Out of 44
400 cyclones that originated over BoB and AS, investigation is carried out on 16 cyclones which
401 are having life time of 4 days or more. The TC centre is fixed based on the best tracks data
402 available from IMD at 3 h intervals. GPS RO overpasses that occurred within the radius of
403 1000 km from the centre of TC are separated. Tropical tropopause parameters are estimated
404 for each individual profiles that occurred at various distances within 1000 km and are
405 grouped for every 250 km radius from the centre of TC. They are further separated based on
406 the intensity of the TC. In order to make quantitative estimates of the effect of TCs on the
407 tropopause parameters, individual tropopause parameters obtained during TC are removed
408 from the climatological mean tropopause parameters that are obtained by averaging the GPS
409 RO measurements available from 2002 and 2013 (CHAMP+COSMIC). The effect of TCs on
410 the vertical distribution of water vapor obtained from COSMIC GPS RO is also investigated.
411 Again GPS RO overpasses that occurred within the radius of 500 km from the TC center
412 within the ± 1 h for every 3h are separated for every 100, 200, 300, 400, and 500 km from the
413 center of the TC. Finally, detailed investigations are made to see the effect of TCs on the
414 tropopause parameters within 500 km from the centre of TC. The main findings of the present
415 study are summarized in the following:

- 416 1. In general, the CPH (LRH) is lowered by 0.6 km (0.4 km) in most of the areas within
417 the 1000 km radius from the TC centre and CPT (and LRT) is colder by 3-4 K. COH
418 has increased up to 2 km and TTL thickness reduced by 2 km within 500 km from the
419 TCs and at some areas up to 1000 km.
- 420 2. CPH (CPT) increases (decreases) as we move away from the TC centre within 500
421 km. There exists a difference of 0.4 km (3 K) in the CPH (CPT) within 500 km from
422 centre of TC. Similar variability in the LRT is observed but not in LRH. An inverse
423 relation between LRH and LRT is noticed but not in CPH and CPT. Nearly 2 km
424 decrease in COH is clearly noticed when we move away from the TC centre leading
425 to the total increase in the TTL thickness of 3 km within 500 km.
- 426 3. The decrease in TTL thickness within 500 km from TC centre is not only because of
427 pushing up of the COH but also decreasing of CPH.
- 428 4. Higher RH is noticed within 500 km from the TC centre reaching as high as 15km.
429 Thus, it is clear that deep convection prevailing within 500 km from the centre of TC
430 can penetrate to the lower stratosphere through the tropopause.
- 431 5. In general, no significant difference in the temperature structure within 500 km from
432 TC centre below 14 km is noticed. However, large variation in the mean temperature
433 structure is noticed above 14 km. There exists a temperature difference of 5K in the
434 UTLS region in the profiles that occur within 100 km from the profiles that occurred
435 away of 400 km.
- 436 6. Multiple tropopause structures are also visible in the profiles that occurred within 100
437 km from the TC.
- 438 7. The colder tropopause temperatures are clearly observed within 1000 km in case of
439 CPT and throughout 1000 km in the eastern side in case of LRT. In general, larger RH
440 values are noticed in the south-eastern side of the TCs in the lower layer (0-5 km) but

441 throughout south side of the TC in the layer 5-10 km. Higher RH values of 70% or
442 more are noticed on the eastern side of TC in the layer 10-15 km. Interestingly COH
443 is much higher over 1000 km and also towards south side from the TC centre with
444 maximum altitude of around 15 km leading to the lesser TTL thickness. TTL
445 thickness is less than 3 km within 500 km from the centre of TC and up to 1000 km in
446 the southern side.

447 Thus, this study clearly demonstrated that the TCs can significantly affect the tropical
448 tropopause and the effects are more pronounced within 500 km from the centre of TC. It will
449 be interesting to see the ozone variability in the upper troposphere and water vapor in the
450 lower stratosphere using satellite observations at the same time and hence STE processes
451 during the TC which will be our future work. Further, in the present study we are unable to
452 make quantitative estimates of the tropopause parameters variability during different stages
453 (time series) of the cyclone due to sparse data of existing GPS RO observations. Once the
454 data is available from the other similar payload (ROSA onboard Megha Tropiques) launched
455 in 2011 in low inclination and forthcoming COSMIC-2, which will have six low earth orbit
456 GPS receivers to be launched in low inclination in the first half of 2016, we can able to
457 quantify the effects more effectively.

458 **Acknowledgements:** We would like to thank TAAC for providing GPS RO data used in the
459 present study through their ftp site. The tropical cyclone best track data used in the present
460 study provided by IMD through their website is highly acknowledged. This work is done as a
461 part of CAWSES India Phase- II Theme 3 fully supported by Indian Space research
462 organization.

463

464 **References:**

- 465 Anthes, R. A., Bernhardt, P. A., Chen, Y., Cucurull, L., Dymond, K. F., Ector, D., Healy, S.
466 B., Ho, S.-H., Hunt, D. C., Kuo, Y.-H., Liu, H., Manning, K., McCormick, C., Meehan, T.
467 K., Randel, W. J., Rocken, C., Schreiner, W. S., Sokolovskiy, S. V., Syndergaard, S.,
468 Thompson, D. C., Trenberth, K. E., Wee, T.-K., Yen, N. L., and Zeng, Z.: The
469 COSMIC/Formosat/3 mission: Early results, *B. Amer. Meteor. Soc.*, 89, 313–333, 2008.
- 470 Biondi, R., Neubert, T., Syndergaard, S., and Nielsen, J. K.: Radio occultation bending angle
471 anomalies during tropical cyclones, *Atmos. Meas. Tech.*, 4, 1053–1060, doi:10.5194/amt-4-
472 1053-2011, 2011.
- 473 Biondi, R., Ho, S. P., Randel, W., Syndergaard, S., and Neubert, T.: Tropical cyclone cloud-
474 top height and vertical temperature structure detection using GPS radio occultation
475 measurements, *J. Geophys. Res. Atmos.*, 118, 5247–5259, doi:10.1002/jgrd.50448, 2013.
- 476 Biondi, R., Steiner, A. K., Kirchengast, G., and Rieckh, T.: A characterization of thermal
477 structure and conditions for overshooting of tropical and extra tropical cyclones with GPS
478 radio occultation, *Atmos. Chem. Phys. Discuss.*, 14, 29395-29428, doi:10.5194/acpd-14-
479 29395-2014, 2014.
- 480 Cairo, F., Buontempo, C., MacKenzie, A. R., Schiller, C., Volk, C. M., Adriani, A., Mitev,
481 V., Matthey, R., Di Donfrancesco, G., Oulianovsky, A., Ravegnani, F., Yushkov, V., Snels,
482 M., Cagnazzo, C., and Stefanutti, L.: Morphology of the tropopause layer and lower
483 stratosphere above a tropical cyclone: a case study on cyclone Davina (1999), *Atmos.*
484 *Chem. Phys.*, 8, 3411– 3426, doi:10.5194/acp-8-3411-2008, 2008.
- 485 Corti, T., Luo, B. P., deReus, M., Brunner, D., Cairo, F., Mahoney, M. J., Matucci, G.,
486 Matthey, R., Mitev, V., dos Santos, F. H., Schiller, C., Shur, G., Sitnikov, N. M., Spelten,
487 N., Vossing, H. J., Borrmann, S., and Peter, T.: Unprecedented evidence for overshooting
488 convection hydrating the tropical stratosphere, *Geophys. Res. Lett.*, 35, L10810,
489 doi:10.1029/2008GL033641, 2008.

490 Danielsen, E. F.: In situ evidence of rapid, vertical, irreversible transport of lower
491 tropospheric air into the lower tropical stratosphere by convective cloud turrets and by
492 larger-scale upwelling in tropical cyclones, *J. Geophys. Res.*, 98, 8665–8681,
493 doi:10.1029/92JD02954,1993.

494 Das, S.S., Venkat Ratnam. M., Uma, K.N., Patra. A.K., Subrahmanyam.K.V., Girach, I.A.,
495 Aneesh.S., Sijikumar. S., Kumar.K.K., Suneeth. K. V., Ramkumar, G.: Stratosphere-
496 troposphere exchange during the tropical cyclone Nilam. *Atmos. Chem. Phys. Discuss.*,
497 2015 (Submitted)

498 Davis, C. A., Ahijevych, D. A., Haggerty, J. A., and Mahoney, M. J.: Observations of
499 Temperature in the Upper Troposphere and Lower Stratosphere of Tropical Weather
500 Disturbances, *J. Atmos. Sci.*, 71, 1593–1608, doi:10.1175/JAS-D-13-0278.1,
501 2014.Emanuel, K. A.: Increasing destructiveness of tropical cyclones over the past 30
502 years, *Nature*, 436, 686–688, doi:10.1038/nature03906, 2005.

503 Emanuel, K. A.: Downscaling CMIP5 climate models shows increased tropical cyclone
504 activity over 21st century, *P. Natl. Acad. Sci. USA*, 110, 12219–12224, 2013.

505 Fueglistaler, S., Dessler, A.E., Dunkerton, T.J., Fu, I., Folkins, Q., Mote, P.W.: Tropical
506 tropopause layer. *Review of Geophysics* 47, RG1004, doi:10.1029/2008RG000267, 2009.

507 Gettelman, A., Forster, P. M. F.: A climatology of the tropical tropopause layer. *Journal of*
508 *Meteorological Society of Japan*, 80, 911–924, doi:10.2151/jmsj. 80.911, 2002.

509 Gettelman, A., Birner, T.: Insights into tropical tropopause layer processes using global
510 models. *Journal of Geophysical Research* 112, D23104, doi:10.1029/2007JD008945, 2007.

511 Highwood, E. J., Hoskins, B. J.: The tropical tropopause. *Quarterly Journal of Royal*
512 *Meteorological Society* 124, 1579–1604, doi:10.1002/qj.49712454911, 1998.

513 Holton, J. R., Haynes, P.H., McIntyre, M.E., Douglass, A. R., Rood, R.B., Pfister, L.:
514 Stratosphere Troposphere exchange. *Reviews of Geophysics* 33, 403–439,
515 doi:10.1029/95RG02097, 1995.

516 Kishore, P., Venkat Ratnam, M., Namboothiri, S.P., Isabella Velicogna, Ghouse Basha,
517 Jiang, J. H., Igarashi, K., Rao, S.V. B., Sivakumar, V.: Global (50°S-50°N) distribution of
518 water vapor observed by COSMIC GPS RO: Comparison with GPS radiosonde, NCEP,
519 ERA-Interim and JRA-25 reanalysis data sets. *Journal of Atmospheric and Solar Terrestrial*
520 *Physics*, 73, 1849–1860, doi:10.1016/j.jastp.2011.04.017, 2011.

521 Koteswaram, P.: On the structure of hurricanes in the upper troposphere and lower
522 stratosphere, *Mon. Weather Rev.*, 95, 541–564, 1967.

523 Krishnamurthy, B. V., Parameswaran, K., Rose, K.O.: Temporal variations of the tropical
524 tropopause. *Journal of Atmospheric Science* 43, 914–922, 1986.

525 Kuo, Y.-H., Wee, T.-K., Sokolovskiy, S., Rocken, W., Schreiner, W., Hunt, H., and Anthes,
526 R.A.: Inversion and Error Estimation of GPS Radio Occultation Data, *J. Meteorol. Soc.*
527 *Jpn.*, 82, 507–531, 2004.

528 Kursinski, E. R., Hajj, G. A., Schofield, J. T., Linfield, R. P., and Hardy, K. R.: Observing
529 Earth's atmosphere with radio occultation measurements using the Global Positioning
530 System, *J. Geophys. Res.*, 102, 23429–23465, 1997.

531 Mehta, S.K., Krishna Murthy, B.V., Rao, D.N., Ratnam, M.V., Parameswaran, K., Rajeev,
532 K., Raju, C.S., Rao, K.G.: Identification of tropical convective tropopause and its
533 association with cold point tropopause. *Journal Geophysical Research* 113, D00B04,
534 <http://dx.doi.org/10.1029/2007JD009625>, 2008.

535 Mehta, S. K., Venkat Ratnam, M., Krishna Murthy, B. V.: Multiple tropopauses in the
536 tropics: A cold point approach. *Journal Geophysical Research*, 116, D20105,
537 doi:10.1029/2011JD016637, 2011.

538 Midya, S. K., Dey, S. S., & Chakraborty, B.: Variation of the total ozone column during
539 tropical cyclones over the Bay of Bengal and the Arabian Sea. *Meteorology and*
540 *Atmospheric Physics*, 117(1-2), 63-71, 2012.

541 Pattnaik, D. R., and Rama Rao, Y. V.: Track Prediction of very sever cyclone ‘Nargis’ using
542 high resolution weather research forecasting (WRF) model, *Journal of earth system science*,
543 118 (4), 309-329, 2008.

544 Penn, S.: Ozone and temperature structure in a Hurricane, *J. Appl. Meteorol.* 4, 212–216,
545 1965.

546 Pommereau, J.-P. and Held, G.: Is there a stratospheric fountain?, *Atmos. Chem. Phys.*
547 *Discuss.*, 7, 8933–8950, doi:10.5194/acpd- 7-8933-2007, 2007.

548 Randel, W. J., Wu, F., Gaffen, D.: Interannual variability of the tropical tropopause derived
549 from radiosonde data and NCEP reanalysis. *Journal Geophysical Research* 105, 15,509–
550 15,524, 2000.

551 Rao, D. N., M. V. Ratnam, Sanjay Mehta, Debashis Nath, S. Ghose Basha, V. V. M.
552 Jagannadha Rao, B. V. Krishna Murthy, T. Tsuda, and Kenji Nakamura.: Validation of the
553 COSMIC radio occultation data over Gadanki (13.48 N, 79.2 E): A tropical region, *Terr.*
554 *Atmos. Oceanic Sci.*, 20, 59–70, doi: 10.3319/TAO.2008.01.23.01(F3C), 2009.

555 Ray, E. A. and Rosenlof, K. H.: Hydration of the upper troposphere by tropical cyclones, *J.*
556 *Geophys. Res.*, 112, D12311, doi:10.1029/2006JD008009, 2007.

557 Reid, G. C. Gage, K.S.: Inter-annual variations in the height of tropical tropopause. *Journal of*
558 *Geophysical Research* 90, 5629–5635, doi:10.1029/ JD090iD03p05629, 1985.

559 Romps, D. M., and Z. M. Kuang, 2009: Overshooting convection in tropical cyclones.
560 *Geophys. Res. Lett.*, 36, L09804, doi:10.1029/ 2009GL037396

561 Santer et al.: Contributions of anthropogenic and natural forcing to recent tropopause height
562 changes. *Science* 301, 5632, 479-483, DOI: 10.1126/science.1084123, 2003.

563 Schreiner, W., C. Rocken, S. Sokolovskiy, S. Syndergaard, and D. Hunt.: Estimates of the
564 precision of GPS radio occultations from the COSMIC/FORMOSAT-3 mission, *Geophys.*
565 *Res. Lett.*, 34, L04808, doi:10.1029/2006GL027557, 2007.

566 Seidel, D. J., Ross, R.J., Angell, J.K., Reid, G.C.: Climatological characteristics of the
567 tropical tropopause as revealed by radiosondes. *Journal of Geophysical Research.*, 106,
568 7857–7878, 2001.

569 Shimizu, A., Tsuda, T.: Variations in tropical tropopause observed with radiosondes in
570 Indonesia. *Geophysical Research Letters* 27, 2541–2544, 2000.

571 Škerlak, B., Sprenger, M., and Wernli, H.: A global climatology of stratosphere–troposphere
572 exchange using the ERA-Interim data set from 1979 to 2011, *Atmos. Chem. Phys.*, 14, 913–
573 937, doi:10.5194/acp-14-913-2014, 2014.

574 Venkat Ratnam, M., Tsuda, T., Shiotoani, M., and Fujiwara, M.: New Characteristics of the
575 Tropical Tropopause Revealed by CHAMP/GPS Measurements, *Scientific Online Letters of*
576 *Atmosphere*, 1, 185-188, doi: 10.2151/sola, 2005.

577 Waco, D. E.: Temperatures and turbulence at tropopause levels over hurricane Beula, *Mon.*
578 *Weather Rev.*, 98, 749–755, 1970.

579 Webster, P. J., G. J. Holland, J. A. Curry, and H.-R.Chang.: Changes in Tropical Cyclone
580 Number, Duration, and Intensity in a Warming Environment, *Science*, 309, 1844–1846,
581 2005.

582 World Meteorological Organization (WMO): Meteorology-A three dimensional science.
583 *WMO Bull.*, 6, 134–138, 1957.

584

585

586 **Figure captions:**

587 **Figure 1.** TC tracks with minimum TC life time 4 days and above used for the present study
588 during 2007 - 2013 over North Indian Ocean. Different colors indicate TCs that occurred
589 in different years.

590 **Figure 2.** (a) IMD observed minimum sea level pressure (MSLP; red line) and maximum
591 wind speed (black line) during TC Nargis. (b) TC centered – composite of NOAA OLR
592 observed on 28 April 2008 along with IMD observed Nargis track (red colour line). White
593 arrows show the wind vectors obtained from ERA-Interim on the same day. White circles
594 show the COSMIC RO observed on the same day. Black circles are drawn to shown the 500
595 km, 1000 km, 1500 km and 2000 km away from TC centers. (c) Climatology of CPH for the
596 month of April obtained while averaging from 2002-2013 and small black circle show the
597 Nargis TC centre observed on 28 April 2008.

598 **Figure 3.** Spatial variation of (a) CPH, (b) LRH, (c) CPT, (d) LRT, (e) COH and (f) TTL
599 thickness with respect to cyclone center Nargis observed on 28 April 2008 for the RO
600 shown in Figure 3b. Black circles are drawn to shown the 250 km, 500 km, 750 km and
601 1000 km away from TC centers.

602 **Figure 4.** Cyclone centered – composite of (a) CPH, (b) LRH, (c) CPT, (d) LRT, (e) COH
603 and (f) TTL thickness observed during the CS and SCS.

604 **Figure 5.** Same as Figure 4 but for the mean difference in the tropopause parameters between
605 climatological mean and individual tropopause parameters observed during TCs
606 (irrespective of cyclone intensity).

607 **Figure 6.** Cyclone centered – composite of averaged RH observed during TCs (irrespective
608 of TC intensity) in the layer (a) 0-5 km, (b) 5-10 km and (c) 10-15 km using COSMIC GPS
609 RO wet-profiles.

610 **Figure 7.** Mean temperature structure observed using GPS RO profiles that occurred within
611 100, 200, 300, 400, and 500 km from the TC centre. Horizontal bars show the standard
612 error. For clarity, the temperature structure observed between 16 km and 18 km is shown in
613 the box.

614 **Figure 8.** Variability in the tropopause parameters of (a) CPH and CPT, (b) LRH and LRT,
615 (c) COH and (d) TTL thickness that observed within 500 km from the centre of TC.
616 Vertical bars show the standard error.

617

618 **Table caption:**

619 Table 1: Cyclone name, grade, cyclone intensity number, period, centre latitude, centre
620 longitude, estimated central pressure, estimated maximum sustained surface wind, estimated
621 pressure drop at the centre of all the cyclones used in the present study provided by IMD.

622

623

624

625 **Table:**

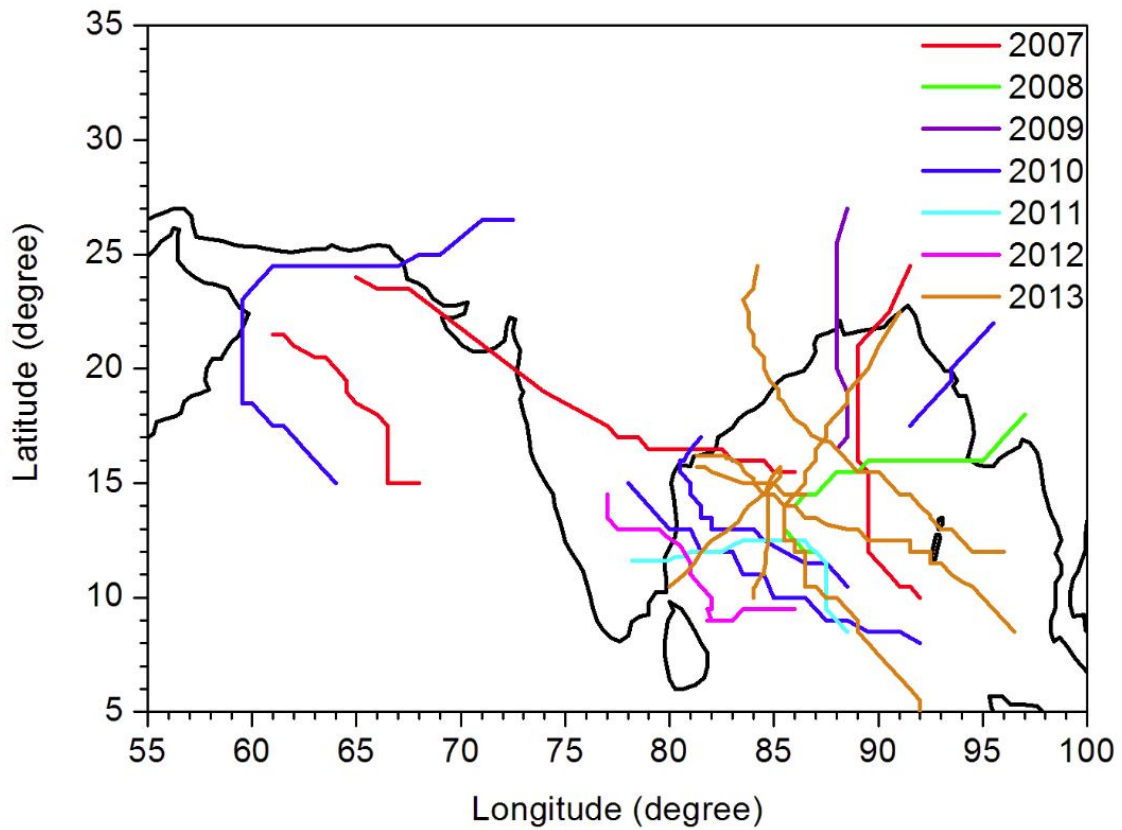
Cyclone Name	Grade	CI.No	Period	Centre latitude	Centre longitude	Estimated Central Pressure (hPa)	Estimated Maximum Sustained Surface Wind (kt)	Estimated Pressure drop at the Centre (hPa)
03B	CS	2.5	21Jun-26Jun 2007	23.5	66	986 (25Jun)	35	6
Gonu	SuCS	6.5	02Jun-07Jun 2007	20	64	920 (04Jun)	127	80
SIDR	VSCS	6	11Nov-16Nov 2007	19.5	89	944 (15Nov)	115	66
Nargis	VSCS	5	27Apr-03May 2008	16	94	962 (02May)	90	40
Aila	SCS	-	23May-26May 2009	22	88	968 (25May)	60	20
Jal	SCS	3.5	04Nov-07Nov 2010	11	84	988 (06Nov)	60	18
Giri	VSCS	5.5	20Oct-23Oct 2010	19.8	93.5	950 (22Oct)	105	52
PHET	VSCS	4.5	31May-06Jun 2010	18.5	60	964 (02Jun)	85	36
Laila	SCS	3.5	17May-21May 2010	14.5	81	986 (19May)	55	15
Thane	VSCS	4.5	25Dec-30Dec 2011	12	81	970 (29Dec)	75	30
Nilam	CS	3	28Oct-01Nov 2012	11.5	81	990 (31Oct)	45	10
Phailin	VSCS	6	08Oct-14Oct 2013	17.1	86.8	940 (11Oct)	115	66
Madi	VSCS	4	06Dec-12Dec 2013	15.4	85.3	988 (10Dec)	65	16
Helen	SCS	3.5	19Nov-22Nov 2013	16.1	82.7	990 (21Nov)	55	17
Mahasen	CS	3	10May-16May 2013	18.5	88.5	990 (15May)	45	10
Leher	VSCS	4	23Nov-28Nov 2013	13.2	87.5	980 (26Nov)	75	26

626 Table 1: Cyclone name, grade, cyclone intensity number, period, centre latitude, centre

627 longitude, estimated central pressure, estimated maximum sustained surface wind, estimated

628 pressure drop at the centre of all the cyclones used in the present study provided by IMD.

629 **Figures:**



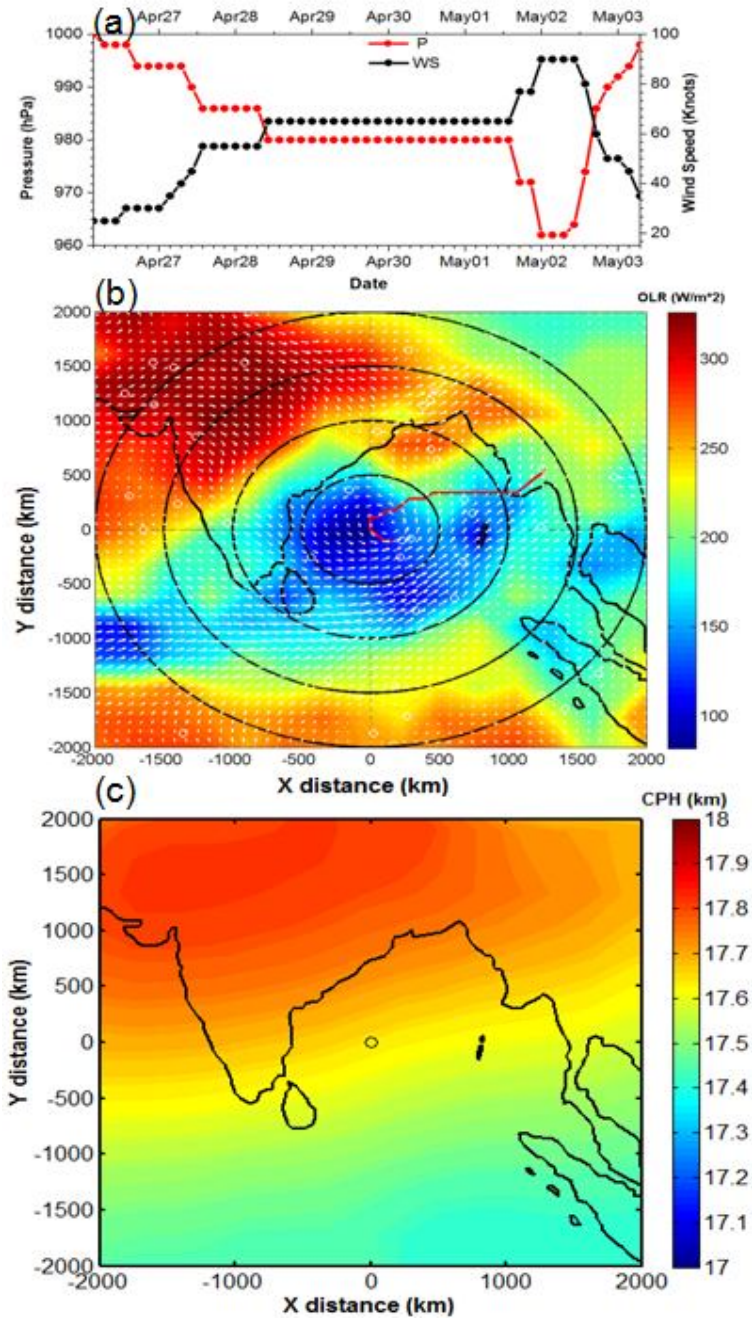
630

631 **Figure 1.** TC tracks with minimum TC life time 4 days and above used for the present study

632 during 2007 - 2013 over North Indian Ocean. Different colors indicate TCs that occurred

633 in different years.

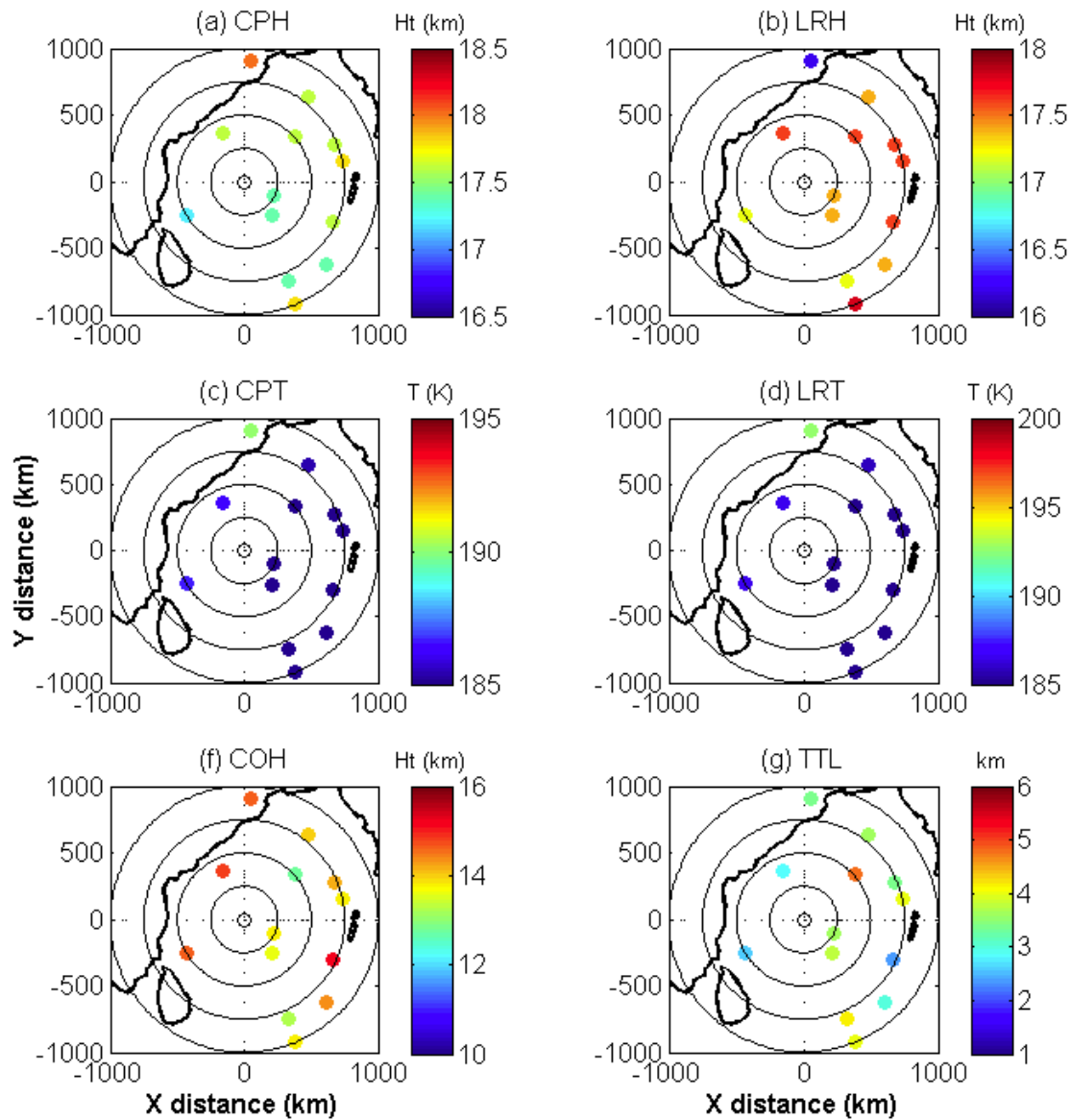
634



635

636 **Figure 2.** (a) IMD observed minimum sea level pressure (MSLP; red line) and maximum
 637 wind speed (black line) during TC Nargis. (b) TC centered – composite of NOAA OLR
 638 observed on 28 April 2008 along with IMD observed Nargis track (red colour line). White
 639 arrows show the wind vectors obtained from ERA-Interim on the same day. White circles
 640 show the COSMIC RO observed on the same day. Black circles are drawn to shown the
 641 500, 1000, 1500 and 2000km away from TC centres. (c) Climatology of CPH for the month
 642 of April and small black circle show the Nargis TC centre for 28 April 2008.

643

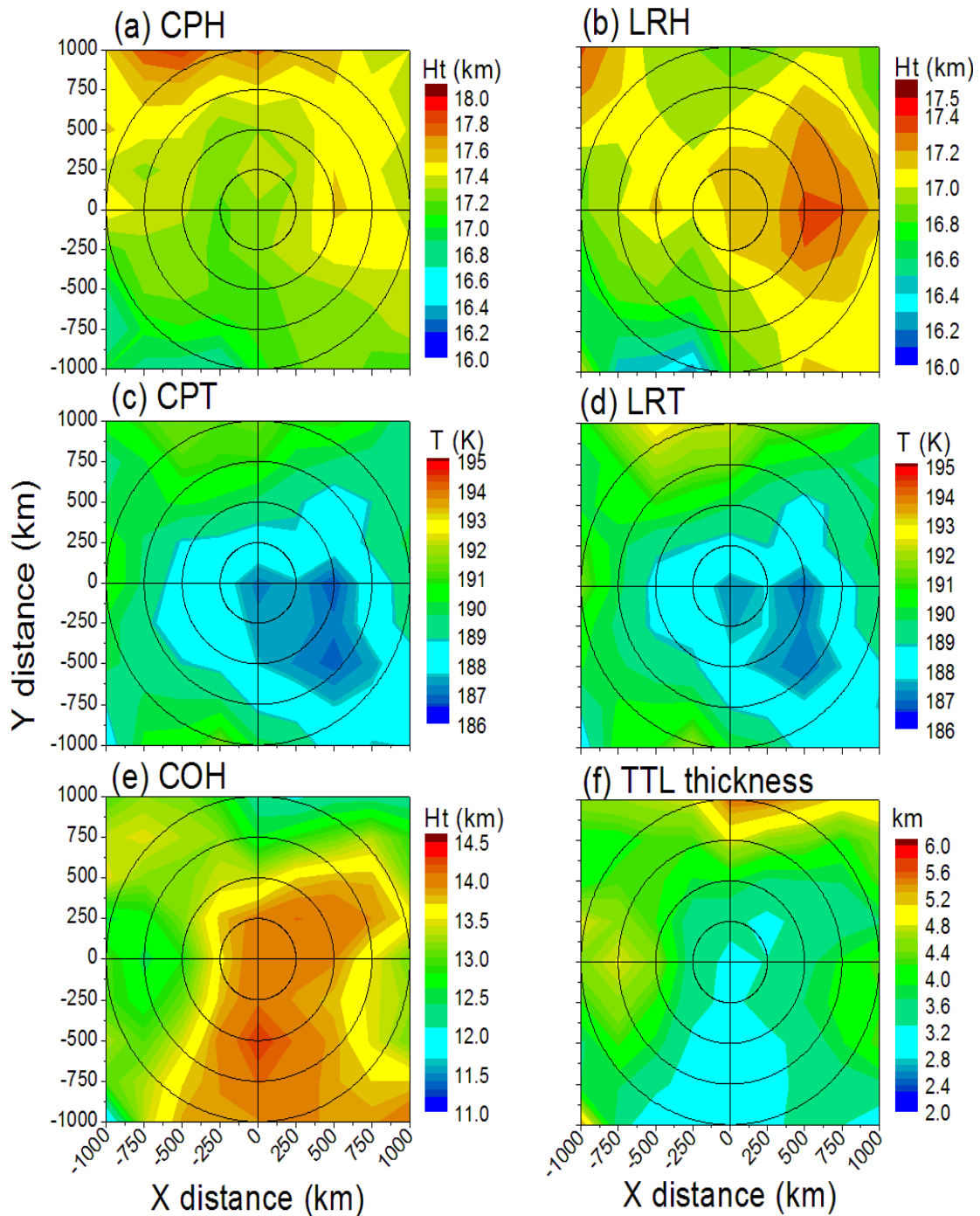


644

645 **Figure 3.** Spatial variation of (a) CPH, (b) LRH, (c) CPT, (d) LRT, (e) COH and (f) TTL
 646 thickness with respect to cyclone center Nargis observed on 28 April 2008 for the RO
 647 shown in Figure 3b. Black circles are drawn to shown the 250 km, 500 km, 750 km and
 648 1000 km away from TC centers.

649

650



651

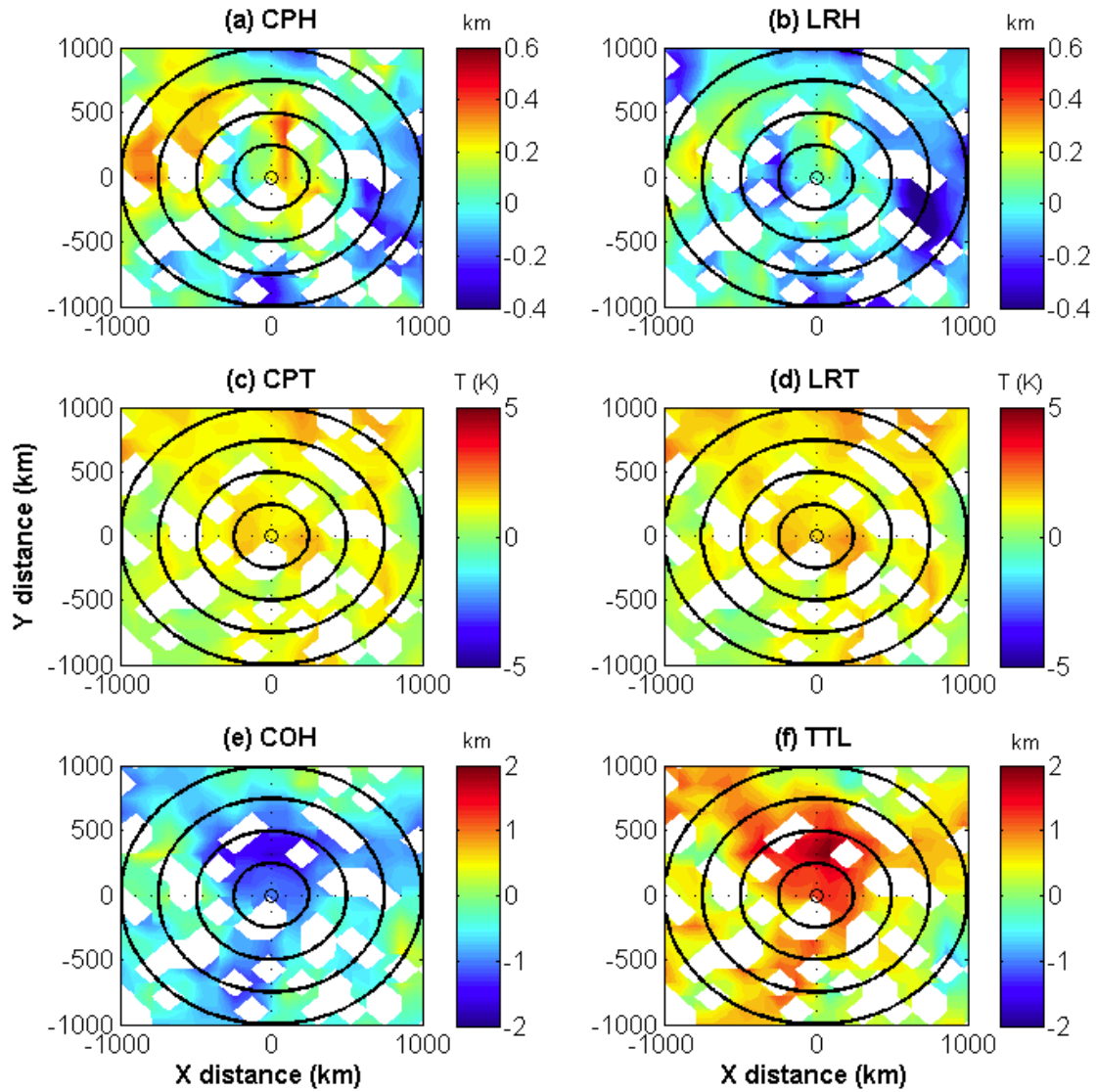
652 **Figure 4.** Cyclone centered – composite of (a) CPH, (b) LRH, (c) CPT, (d) LRT, (e) COH

653 and (f) TTL thickness observed during the CS and SCS. Black circles are drawn to shown

654 the 250 km, 500 km, 750 km and 1000 km away from TC centers.

655

656

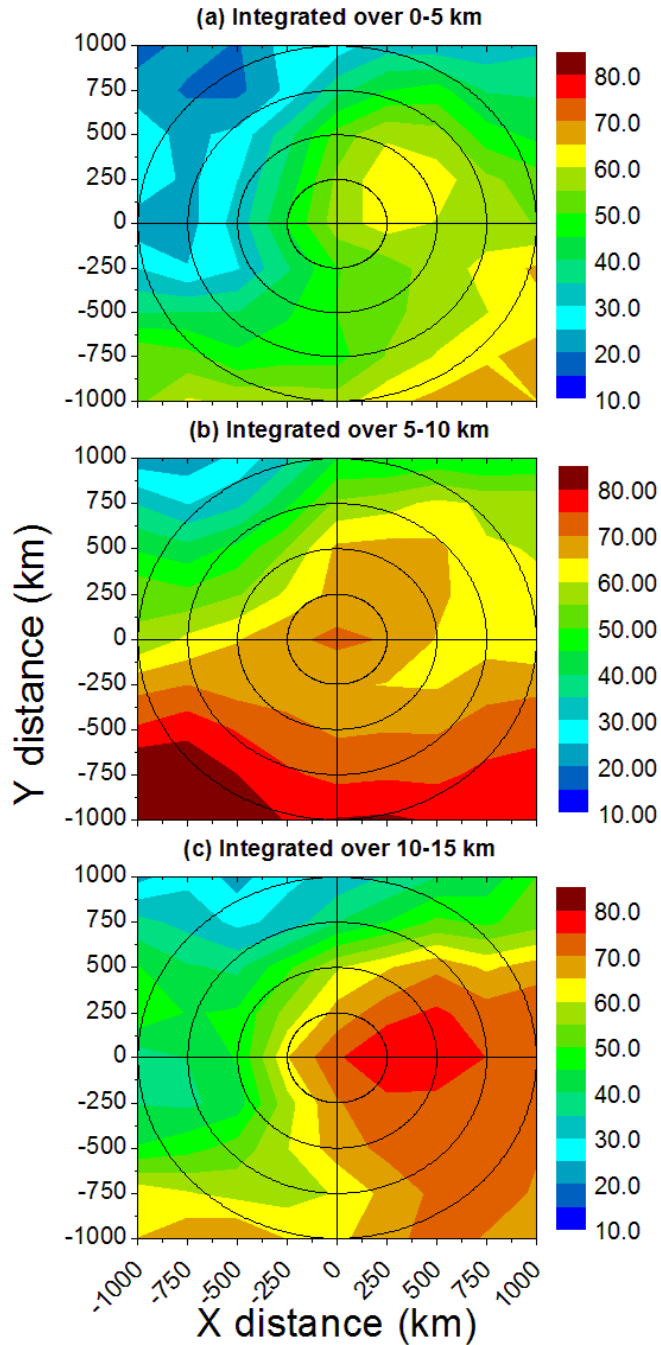


657

658 **Figure 5.** Same as Figure 4 but for the mean difference in the tropopause parameters between
 659 climatological mean and individual tropopause parameters observed during TCs
 660 (irrespective of cyclone intensity).

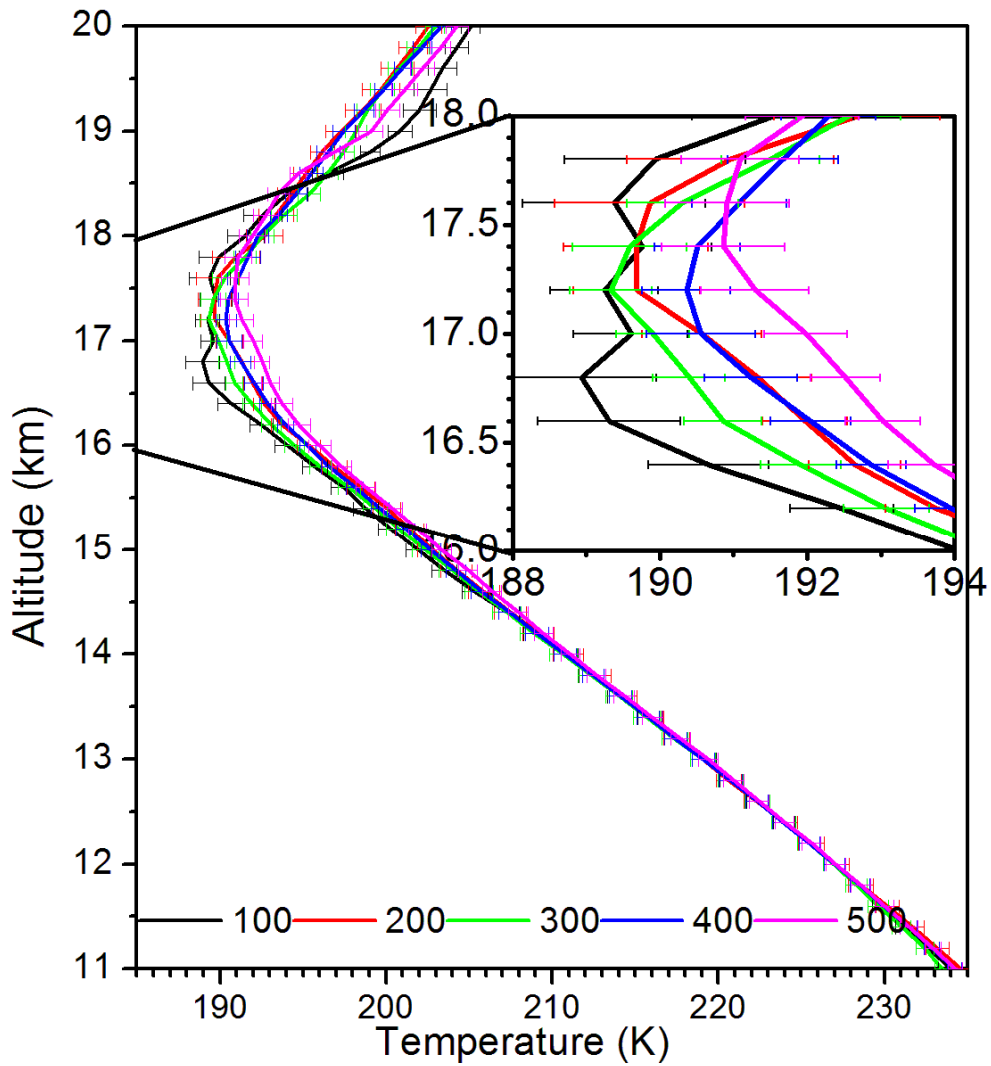
661

662



663

664 **Figure 6.** Cyclone centered – composite of averaged RH observed during TCs (irrespective
 665 of TC intensity) in the layer (a) 0-5 km, (b) 5-10 km and (c) 10-15 km using COSMIC GPS
 666 RO wet-profiles. Black circles are drawn to shown the 250 km, 500 km, 750 km and 1000
 667 km away from TC centers.



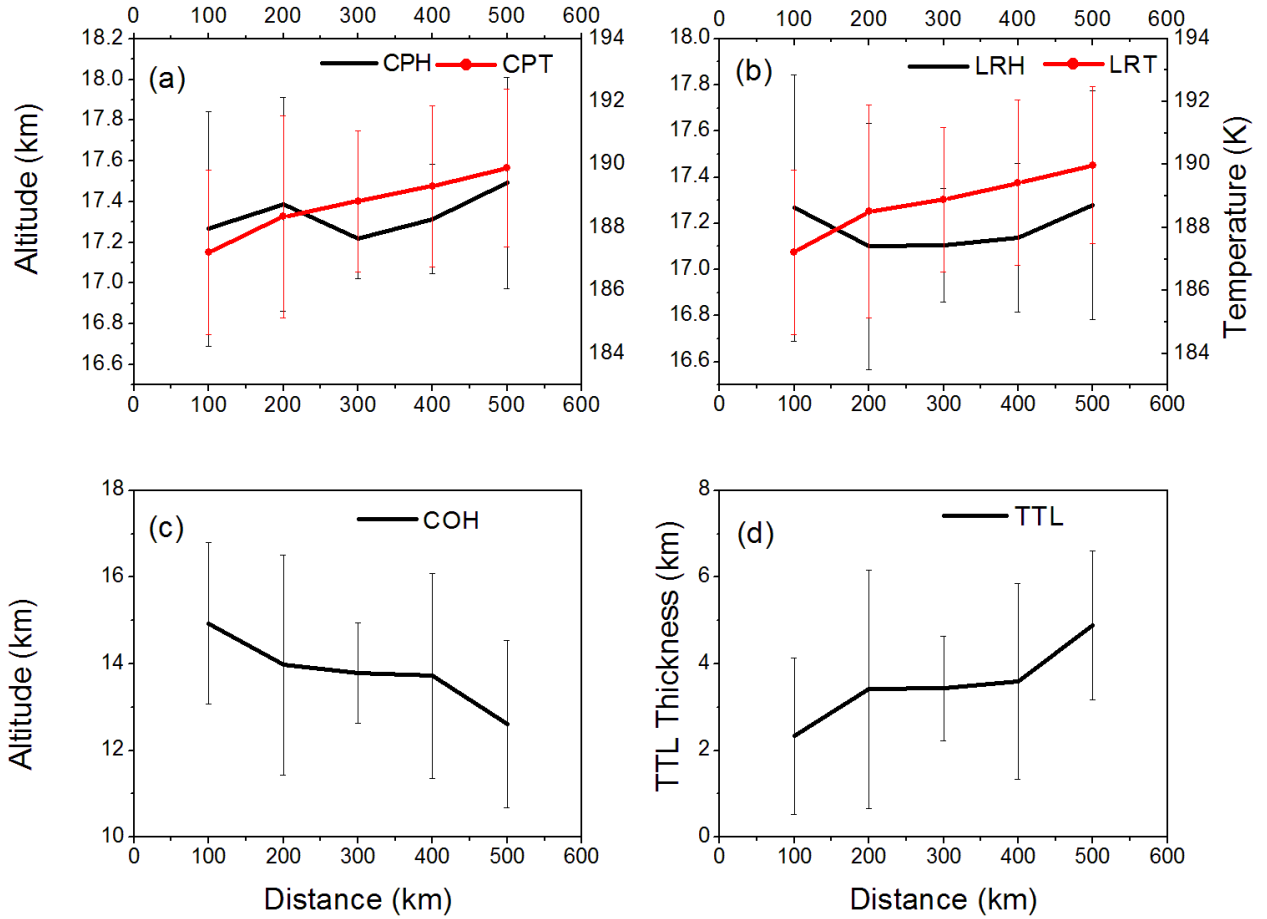
668

669 **Figure 7.** Mean temperature structure observed using GPS RO profiles that occurred within
 670 100, 200, 300, 400, and 500 km from the TC centre. Horizontal bars show the standard
 671 error. For clarity, the temperature structure observed between 16 km and 18 km is shown in
 672 the box.

673

674

675



676

677

678 **Figure 8.** Variability in the tropopause parameters of (a) CPH and CPT, (b) LRH and LRT,
 679 (c) COH and (d) TTL thickness that observed within 500 km from the centre of TC.

680 Vertical bars show the standard error.

681

682